Plasma Effects on Electromagnetic Wave Scattering in Suborbital Hypersonic Flight

Salvatore Esposito
Dipartimento di Elettronica e Telecomunicazioni (DET)
Politecnico di Torino
Torino, Italy
salvatore_esposito@polito.it

Domenic D'Ambrosio
Dipartimento di Ingegneria Meccanica e Aerospaziale (DIMEAS)
Politecnico di Torino
Torino, Italy
domenic.dambrosio@polito.it

Giuseppe Vecchi
Dipartimento di Elettronica e Telecomunicazioni (DET)
Politecnico di Torino
Torino, Italy
giuseppe.vecchi@polito.it

Andrea Scarabosio
LINKS foundation
Torino, Italy
andrea.scarabosio@linksfoundation.com

***Abstract*—This paper investigates the impact of plasma generated by a suborbital hypersonic vehicle on electromagnetic wave scattering. Hypersonic flight presents unique challenges due to the complex physical phenomena involved. The high speeds of hypersonic vehicles result in the transfer of kinetic energy to the air through a detached shock wave, leading to heating, compression, and chemical reactions within the flow field. Under certain conditions, ionization phenomena occur, generating a plasma field around the aircraft. This study focuses on calculating the radar cross-section (RCS) of a hypersonic glide vehicle (HGV) at different Mach numbers and suborbital altitudes to understand how the plasma field affects electromagnetic wave propagation and scattering. Computational Fluid Dynamics (CFD) is employed to determine plasma properties such as the electron plasma frequency, collision frequency, and permittivity. Two approaches – an approximate asymptotic method based on Ray Tracing and a Full-Wave method using Finite-Difference Time-Domain (FDTD) – are utilized to assess the impact of the plasma envelope on radar response. The results provide valuable insights into the interaction between the hypersonic plasma field and electromagnetic waves.**

***Index Terms*—Hypersonic plasma, plasma scattering, Hypersonic Glide Vehicle**

I. Introduction

Hypersonic flight presents one of the most complex challenges in aeronautics due to the numerous physical phenomena that occur under these conditions. The high velocity of hypersonic vehicles leads to the transfer of their significant kinetic energy to the surrounding air through a detached shock wave. As a result, the air undergoes heating and compression, exhibiting entirely different phenomena compared to supersonic and subsonic flight regimes. The elevated air temperature triggers chemical reactions within the flow field, resulting in the formation of new chemical species. Additionally, when the speed and altitude conditions are suitable, the shock intensity is sufficient to induce ionization, generating charged particles within the flow field, known as plasma [1]. The hypersonic plasma field that envelops the aircraft and forms in its wake influences the propagation of electromagnetic waves within it. The concentration of charged particles in the flow field can reach several GHz, causing complete blocking and reflection of electromagnetic waves (known as the cut-off condition) [2].

The objective of this study is to investigate the impact of plasma generated by a suborbital hypersonic vehicle on electromagnetic wave scattering. An analysis campaign is conducted to calculate the radar cross-section (RCS) of a hypersonic glide vehicle (HGV) at various Mach numbers and suborbital altitudes. Specifically, altitudes ranging from 30 to 50 km and Mach numbers between 10 and 15 are considered. These ranges are chosen because at lower altitudes, the flight regime is highly collisional, with significant collision frequencies, while at higher altitudes, the thermochemical activity is minimal for these Mach numbers and geometrical configuration.

The geometry of the hypersonic glider is inspired by a waverider configuration, which provides a solid foundation for studying plasma formation around slender bodies during atmospheric hypersonic flight. The results of these analyses, including the plasma electron frequency, plasma collision frequency, and permittivity, are utilized to investigate the RCS. Two approaches are adopted to assess the impact of the plasma envelope on radar response: the first one is an approximate asymptotic method based on ray tracing, while the second is a full-wave method using Finite-Difference Time-Domain (FDTD) techniques.

II. Physical Model

A. Aerothermodynamic model

To proceed with the study of RCS, it is necessary to first evaluate the characteristics of the flow field and the concentrations of various chemical species in order to compute the properties of the plasma field, such as electron plasma frequency, collision frequency, and permittivity. In the context of suborbital flight, the air is modeled as a continuous fluid

Fig. 1. The hypersonic glider geometry.

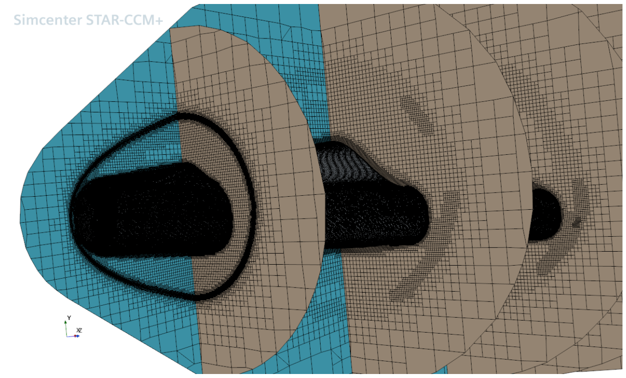

Fig. 2. Example of Adaptive Mesh Refinement.

described by the Navier-Stokes equations. The air is considered a compressible, viscous, and chemically reactive mixture composed of seven species: oxygen (O_2), nitrogen (N_2), nitrogen oxide (NO), atomic nitrogen (N), atomic oxygen (O), nitrogen oxide ions (NO^+), and electrons (e^-). Regarding thermochemical activities, the model considers vibrational and electronic energy in non-equilibrium conditions, as well as chemical reactions and ionization. The thermodynamic and transport characteristics of individual species are derived from [3], while the chemical reactions and their related reaction rates are taken from [4], [5]. A two-temperature model is used to model non-equilibrium energy phenomena [6].

The CFD analyses are performed using the commercial software Metacomp ICFD++ [7]. All analyses are conducted at an angle of attack of 6°, which exhibits the maximum aerodynamic efficiency for a body of this type [8]. A non-catalytic, radiative adiabatic wall is assumed. The phenomena to be described not only make the problem complex but also computationally demanding. Considering that most of the thermochemical activities occur in the region near the nose of the glider, where the shock wave is normal to the flow direction and thus more intense, a high degree of accuracy in that area is crucial. However, the curvature radius of the nose is approximately 8 cm, while the overall length of the waverider is about 4 m. To reduce the number of grid points, adaptive mesh refinement based on the Mach number gradient has been employed for each analysis, providing accurate descriptions of the regions at the shock wave.

B. Plasma properties and EM waves propagation models

Regarding the plasma, it is assumed to remain stationary. However, electromagnetic waves exhibit a time dependence expressed as $e^{i\omega t}$, where $\omega = 2\pi f$ represents the angular frequency corresponding to the frequency f. In this model, the focus is on frequencies where the plasma response is dominated by the motion of electrons while considering the effects of electron collisions with neutral species. Additionally, since the phase velocities of the wave are much greater than the thermal velocity of the plasma, a cold plasma model is adopted. This model assumes that the dispersion relation is independent of temperature, and higher-order collective kinetic phenomena are neglected. Under the specific conditions of hypersonic flight where the plasma is non-magnetized and inhomogeneous, the constitutive relationship for permittivity is well described by the Drude model [2]:

$$\begin{aligned} \epsilon_r(\mathbf{r}) &= 1 - \frac{\omega_p^2(\mathbf{r})}{(\omega(\omega - i\nu_c(\mathbf{r}))} \\ &= 1 - \frac{\omega_p^2(\mathbf{r})}{(\omega^2 + \nu_c^2(\mathbf{r}))} + i\frac{\omega_p^2(\mathbf{r})\nu_c}{\omega(\omega^2 + \nu_c^2(\mathbf{r}))} \end{aligned} \tag{1}$$

In this equation, ω represents the angular frequency of the electromagnetic (EM) wave, while ω_p stands for the electron plasma frequency, which depends on the number density of electrons and is described by the following relationship:

$$\omega_p(\mathbf{r}) = \sqrt{\frac{n_e(\mathbf{r})e^2}{m_e\epsilon_0}} \tag{2}$$

Here, n_e is the electron number density, e is the electron charge, m_e is the electron mass, and ϵ_0 is the vacuum permittivity. ν_c is the neutral plasma collision frequency [9]:

$$\nu_c(\mathbf{r}) = \sum_{i=1}^{N} n_i(\mathbf{r})\sigma_{i,e}\sqrt{\frac{8k_bT_e(\mathbf{r})}{\pi m_e}} \tag{3}$$

In Eq.(3), T_e represents the electron temperature, n_i is the neutral number density of the i-th species, $\sigma_{i,e}$ is the neutral-electron scattering cross-section for the neutral species i, and k_b is the Boltzmann constant. The neutral-electron scattering cross-sections are taken from [3].

Under suitable Mach and altitude conditions, the electron number density can reach a level where the plasma frequency is equal to or greater than the EM wave frequency. In such cases, with sufficiently low collision frequencies, the real part of the permittivity can become zero or even negative. As a result, the EM wave becomes evanescent, and its intensity exponentially decreases as it propagates through the plasma. Consequently, the surface of the object is effectively replaced by plasma, which distorts the radar trace by reflecting the radiation. Furthermore, even if the cutoff conditions are not met, refraction and absorption can still occur, causing a redistribution of electromagnetic waves and a decrease in re-radiation.

Two distinct methods are employed to address the challenge of wave propagation in plasma and assess RF scattering (RCS), with a comparative analysis between them where possible:

- Ray-tracing [10]: This is an asymptotic optical method that adopts the Eikonal Ansatz to approximate propagation in the plasma region, while accurately computing the fields just outside through the Radiation Integral [11]–[13]. By decomposing the initial source or pattern into plane waves carried by individual rays, this method effectively handles the propagation within the plasma envelope and the reflection on the aircraft's surface. This approach is particularly valuable when studying large domains, as it allows for the analysis of electromagnetic wave scattering in the wake of the aircraft and the assessment of how the plasma field influences wave propagation. To implement this approach, a custom code has been developed.
- Full-wave technique: These approaches involve numerically solving Maxwell's equations without any approximations. Among full-wave techniques, the Finite-Difference Time-Domain (FDTD) method is utilized mostly in the low EM frequency regime due to its flexibility and relatively low computational cost, particularly in terms of memory requirements compared to other methods [14]. For this method, the commercial software CST has been employed [15].

III. Preliminary Results

Here, we present the results of a CFD analysis for a Mach number of 15 and an altitude of 40 kilometers. The results for this case are particularly significant due to the high thermodynamic activity and low collisionality that characterize these conditions. Specifically, Figs. 3 and 4 show that the highest values of plasma frequency and collision frequency are observed in the nose region, where temperatures are the highest and the shock wave is normal to the flow direction. In Fig. 3, plasma frequencies exceeding 1 GHz are not only present in the nose region but also on the underside of the body and in the wake. This distribution is attributed to the convective transport of newly formed electron fluid from the nose region along the body and downstream into the wake. By observing Fig. 4, it can be noted that this specific Mach and altitude condition is characterized by low neutral collisionality. When considering an electromagnetic wave frequency of 1 GHz, Fig. 5 reveals that the real part of the permittivity reaches negative values even in the wake, indicating the occurrence of a cut-off phenomenon in a region much larger than just the aircraft itself.

Fig.6 and fig.7 show the results obtained by applying the ray tracing to calculate a bistatic RCS. This method is useful for conducting analyses on large volumes and, in this case, for visualizing the effects of plasma in the wake. The results are shown for rays incident from below at 45° from vehicle main axis as shown in fig. 6 (here main vehicle axis coincides with x-axis). The rays, calculated for a EM frequency of 1GHz, strongly refracted by the plasma are depicted in red, while the rays in the absence of plasma are shown in blue. Observing the color map of the real part ϵ_r for $z = 0$, it is evident how the non-homogeneity of the permittivity field in the plasma wake as near the main body generates the "force" deflecting the rays.

Fig. 6 also displays the plasma frequency in a section within the y-z plane towards the rear of the aircraft. It is evident that

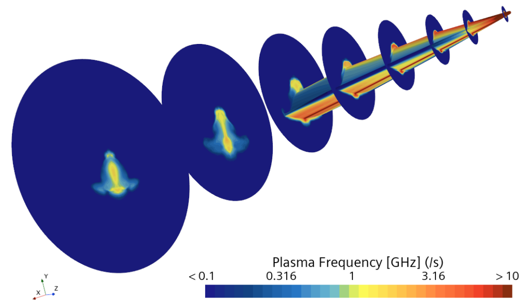

Fig. 3. Plasma frequency at Mach 15 and 40 km altitude.

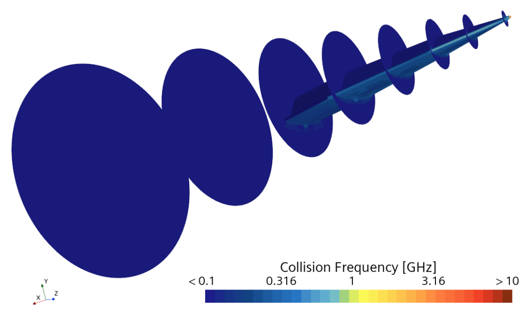

Fig. 4. Collision frequency at Mach 15 and 40 km altitude.

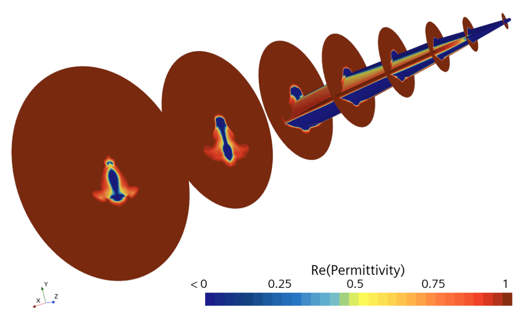

Fig. 5. Real part of permittivity at Mach 15 and 40 km, with a frequency of the EM wave, f=1 GHz.

this region of high density is separated from the lower surface and partially extends in the aerodynamic wake. These red rays clearly demonstrate substantial deviation or even reflection from the vicinity of this high density plasma regions. The RCS (Radar Cross Section) as a function of the observation angle is shown in Fig.7. The inset illustrates the geometry of the observation and incidence angles with respect to the aircraft, both at a 45° aspect angle. The case with plasma (solid line) is compared to the case in vacuum space (dashed line). The vacuum case shows the forward or "refracted" peak at $\theta = 45$ and the reflected peak at $\theta = 135$. The backscattering region (negative θ with monostatic RCS at θ=-135°) is flat around the value of -10 dBsm. The differences with the plasma case are evident, particularly for the (larger) refracted peaks while the reflected peak is broadened and a new reflected peak appears at around θ=90°. This latter is thought to be connected with high density plasma region below and in the rear of the vehicle. Regarding radar return (in this geometry at θ=-135°), the plasma augmented the RCS by approximately 6 dBsm. Similar or larger effects are expected for lower frequencies.

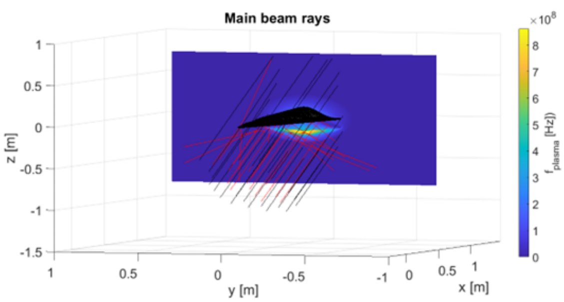

Fig. 6. Rays with a 45° angle of incidence in presence of Plasma.

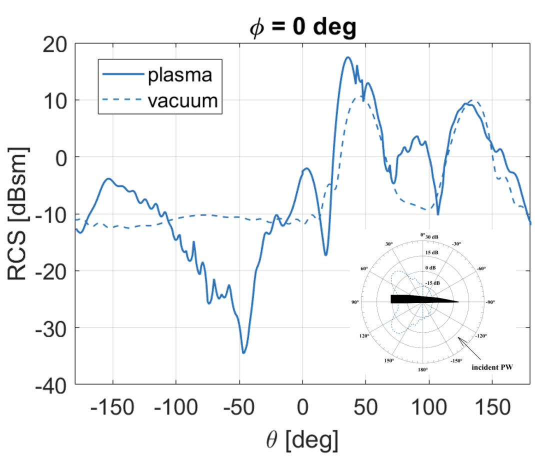

Fig. 7. Comparison of bistatic RCS with plasma and in vacuum.

In the final version of the paper, we will present all the results related to the RCS study, including comparisons across different electromagnetic frequency regimes and various Mach and altitude conditions.

Acknowledgments

This research was conducted under the financial support provided by the PON (Programmi Operativi Nazionali) research funds. We are grateful to the Italian Ministry of Education, University and Research (MIUR) for managing the PON funding program and for supporting our research endeavors.

References

[1] J. D. Anderson, "Hypersonic and High Temperature Gas Dynamics," AIAA, 1989.

[2] T. H. Stix, "Waves in plasmas," Springer Science & Business Media, 1992.

[3] R. N. Gupta, J. M Yos, R. A. Thompson, and K. Lee, "A review of reaction rates and thermodynamic and transport properties for an 11-species air model for chemical and thermal nonequilibrium calculations to 30000 K," (1990).

[4] C. Park,"Review of chemical-kinetic problems of future NASA missions. I-Earth entries," Journal of Thermophysics and Heat transfer 7.3 (1993): 385-398.

[5] C. Park, R. L. Jaffe, and H. Partridge, "Chemical-kinetic parameters of hyperbolic earth entry," Journal of Thermophysics and Heat transfer 15.1 (2001): 76-90.

[6] P. A. Gnoffo, "Conservation equations and physical models for hypersonic air flows in thermal and chemical nonequilibrium," Vol. 2867. National Aeronautics and Space Administration, Office of Management, Scientific and Technical Information Division, 1989.

[7] S. Chakravarthy, O. Peroomian, U. Goldberg, and S. Palaniswamy, "The CFD++ computational fluid dynamics software suite," AIAA and SAE, 1998 World Aviation Conference. 1998.

[8] Y. Ma, T. Yang, Z. Feng, and Q. Zhang, "Hypersonic lifting body aerodynamic shape optimization based on the multiobjective evolutionary algorithm based on decomposition," Proceedings of the Institution of Mechanical Engineers, Part G: Journal of Aerospace Engineering 229.7 (2015): 1246-1266.

[9] Landau, L. D., and E. M. Lifshitz. "Chapter I – The fundamental principles of statistical physics." Course of Theoretical Physics 1980 (1980): 1-33.

[10] A. Scarabosio, et al. "Radiation and scattering of EM waves in large plasmas around objects in hypersonic flight," IEEE Transactions on Antennas and Propagation 70.6 (2022): 4738-4751.

[11] M. Born, and E. Wolf, "Principles of optics: electromagnetic theory of propagation, interference and diffraction of light," Elsevier, 2013.

[12] Y.A. Kravtsov,and I. O. Yuri, "Geometrical optics of inhomogeneous media," Vol. 38. Berlin: Springer-Verlag, 1990.

[13] H. Bremmer, and S. W. Lee, "Propagation of a geometrical optics field in an isotropic inhomogeneous medium," Radio science 19.01 (1984): 243-257.

[14] J. M. Jin, "Theory and computation of electromagnetic fields," John Wiley & Sons, 2015.

[15] SOLVERS, Electromagnetic Simulation; COMPATIBILITY, C. CST Studio Suite. https://www. 3ds. com/ko/products-services/simulia/products/cst-studio-suite/solvers/(accessed on 23 November 2022). doi, 2020, 10: s19051212.